

# Application of Bayesian robust design model to assess the impacts of a hurricane on shorebird demography

DANIEL GIBSON <sup>1,†</sup> THOMAS V. RIECKE,<sup>2</sup> TIM KEYES,<sup>3</sup> CHRIS DEPKIN,<sup>3</sup> JAMES FRASER,<sup>1</sup> AND DANIEL H. CATLIN<sup>1</sup>

<sup>1</sup>Department of Fish and Wildlife Conservation, Virginia Polytechnic Institute and State University, Blacksburg, Virginia 24060 USA

<sup>2</sup>Program in Ecology, Evolution and Conservation Biology, Department of Natural Resources and Environmental Science, University of Nevada Reno, Mail Stop 186, Reno, Nevada 89557 USA

<sup>3</sup>Georgia Department of Natural Resources, 1 Conservation Way, Brunswick, Georgia 31520 USA

**Citation:** Gibson, D., T. V. Riecke, T. Keyes, C. Depkin, J. Fraser, and D. H. Catlin. 2018. Application of Bayesian robust design model to assess the impacts of a hurricane on shorebird demography. *Ecosphere* 9(8):e02334. 10.1002/ecs2.2334

**Abstract.** The increasing use of Bayesian inference in population demography requires rapid advancements in modeling frameworks to approach the rigor and flexibility of the current suite of maximum-likelihood models. We developed an unbiased, Jolly–Seber robust design (JSRD) model that is both accessible and generalizable in a Bayesian hierarchical multistate framework. We integrated band and age-classification data to estimate site entry, temporary emigration, and apparent survival rates, as well as estimate age-class specific abundances. The complete model parameterization is provided in the Appendix S1, as well as tools for simulating capture histories and an assessment of model fit. We applied this model to determine whether these demographic processes in non-breeding population of American oystercatchers (*Haematopus palliatus*) were affected by a major hurricane event (Hurricane Matthew) in coastal Georgia. The JSRD model was demonstrably unbiased at relatively small sample sizes, and the majority of parameters were identifiable in the fully saturated model parameterization. In the model application, we found that Hurricane Matthew temporarily altered local population abundances of American oystercatchers through increased movements of individuals into and out of the observable population, but mortality rates were largely unaffected. Together, our results suggest that American oystercatchers were largely able to avoid the immediate demographic consequences (i.e., reduced survival) of Hurricane Matthew. Integrating age and band ratios from survey data allowed for more descriptive and potentially less biased estimates of age-specific abundance, relative to estimates generated solely from either mark–resight or survey data.

**Key words:** age ratios; American oystercatchers; Bayesian population modeling; hurricanes; Jolly–Seber robust design; non-breeding demography; temporary emigration.

**Received** 30 January 2018; revised 23 May 2018; accepted 24 May 2018. Corresponding Editor: Lucas Joppa.

**Copyright:** © 2018 The Authors. This is an open access article under the terms of the Creative Commons Attribution License, which permits use, distribution and reproduction in any medium, provided the original work is properly cited.

† **E-mail:** gibsond@vt.edu

## INTRODUCTION

Understanding how populations change in abundance across space and time is the underlying goal of many ecological studies. Capture–mark–recapture (CMR) is a well-established approach for estimating the rates and drivers of population changes in wild populations (Lebreton et al. 1992). Parameter estimates from many types

of CMR models, however, are the products of multiple biologically informative or uninformative processes (e.g., apparent survival is the product of site fidelity and survival), which are both of biological interest. Recent advancements have provided researchers with tools to decouple previously confounded variables using ancillary data (Barker 1997, White et al. 2006, Kendall et al. 2013) or through restrictions when individuals

can enter and leave the population (Kendall et al. 1997). The increasing use of Bayesian inference in demographic estimation requires rapid advancements in modeling frameworks to approach the diversity of the maximum-likelihood toolbox. For example, there was no unbiased and accessible robust design estimator in a Bayesian framework until recently (T. V. Riecke et al., *unpublished manuscript*), which inhibited estimation of key demographic processes (Kendall et al. 1997) under realistic model constraints. Although the robust design was originally developed to assess the influence of bias in the observational process on demographic rates of interest (Pollock 1982), it has since been expanded to estimate a series of biologically important demographic rates, including site dispersal rates or temporary emigration (i.e., temporary absence from a study system), using meta- or open-population models (Kendall and Bjorkland 2001, Chabanne et al. 2017). Bayesian robust design alternatives have been published (Link and Barker 2010, Schofield and Barker 2011, Rankin et al. 2016), but they relied heavily on the constraints placed on the prior information for certain parameters, were overly complex, or, most critically, did not produce unbiased or fully identifiable parameter estimates (T. V. Riecke et al., *unpublished manuscript*).

Although confounded with the observation process in many CMR models, temporary emigration can be of biological interest, as it often can be interpreted as breeding behavior or propensity (Muths et al. 2006, Souchay et al. 2014). However, depending on the relative timing and location of the study, temporary emigration may also represent other biologically interesting processes, such as seasonal occupancy rates and shifts in habitat use related to environmental conditions (Sprogis et al. 2016, Chabanne et al. 2017). As temporary emigration often implies a shift in an individual's life-history state (e.g., breeding/non-breeding, migratory/resident), models that explicitly allow for temporary emigration provide a mechanism to assess the fitness consequences of variation in life-history strategies (Blomberg et al. 2013, Weithman et al. 2017).

Intense, large-scale weather phenomena (e.g., hurricanes, wildfires) can alter population trajectories (Frederiksen et al. 2008). However, it is uncertain whether shifts in population size are a direct result of weather or indirectly related

through a shift in ecological function of the surrounding landscape due to the weather event (James et al. 1997, Chu-Agor et al. 2012) or human actions aimed to restore function (e.g., coastal defense, recreational use; Convertino et al. 2011a). Additionally, it remains unclear the extent to which organisms can detect and react to the various weather phenomena. For individuals capable of relatively large movements over short periods, moving, either temporarily or permanently, from dangerous environmental conditions seems like a successful strategy to improve the likelihood of survival (Hong et al. 2018). For example, onset of migration often occurs during periods of favorable weather conditions (Volkov et al. 2016, Le Corre et al. 2017); however, hurricanes and other potentially unfavorable weather events can disrupt migratory behavior (Boone 2016).

Hurricane Matthew resulted in substantial destruction and loss of human life throughout the Caribbean and southeast Atlantic Coast of the United States from 28 September to 10 October 2016. Although islands in the Caribbean experienced the most intense hurricane conditions, Hurricane Matthew's trajectory was peculiar as it struck Georgia directly, which tends to be more sheltered from hurricanes, relative to surrounding states (Keim and Muller 2007). During Hurricane Matthew, coastal Georgia experienced sustained winds of 120 km/h with gusts up to 154 km/h, upwards of 45 cm of rainfall, and a storm surge of 2.34 m, the largest recorded by Hurricane Matthew in the United States (Stewart 2017). American oystercatcher (*Haematopus palliatus*) migration was well underway prior to the arrival of Hurricane Matthew, and large numbers of individuals were moving to or through Georgia and their seasonal non-breeding habitat.

To more effectively capture the potential impacts of an extreme weather event on local population dynamics of a migratory bird, we developed a generalizable Jolly-Seber robust design model (JSRD) parameterized in a Bayesian hierarchical multistate framework. This approach allowed for an assessment of the extent to which Hurricane Matthew influenced various demographic rates (e.g., apparent survival, temporary emigration, entry rates) or abundance measurements (e.g., local population size, off-site population size) for a population of American oystercatchers at a dynamic stopover and overwintering site in coastal

Table 1. Notations and definitions for important parameters used in the Jolly–Seber robust design model.

Notation	Definition
$b_i$	The proportion of individuals that entered the observable population in primary period $i$ , relative to the number of individuals in the data set ( $n$ )
$\beta_i$	The proportion of individuals that entered the observable population in primary period $i$ , relative to the number of individuals in the data set ( $n$ ) that have not entered the observable population by primary period $i$
$\phi_i$	The probability an individual that has entered the observable population by primary period $i$ , survives until primary period $i + 1$
$\gamma''_i$	The probability an individual is available for detection in primary period $i$ , given that it was available for detection in primary period $i - 1$
$\gamma'_i$	The probability an individual is available for detection in primary period $i$ , given that it was not available for detection in primary period $i - 1$
$p_{i,j}$	The probability an individual was detected in sample $j$ of primary period $i$ , conditioned on being both alive and in the observable population
$p_i^*$	The probability an individual was detected at least once during primary period $i$ , conditioned on being both alive and in the observable population

Georgia. We also incorporated age data from photographs of flock surveys into the general demographic model to estimate variation in age-specific abundances among sites and throughout the non-breeding season and demonstrate the flexibility of our model.

## MATERIALS AND METHODS

### Model formulation

We generally follow the model formulation and notation of the open-population robust design (OPRD) model specified by Kendall and Bjorkland (2001) and the multistate Jolly–Seber superpopulation model (Kéry and Schaub 2012) that formed the basis of this model. The theory and applicability of the OPRD model were described in Kendall and Bjorkland (2001), in which they define the model's estimated and derived parameters. However, we provide an abridged list of parameter notation and definitions to assist readers (Table 1). The JSRD model described below deviated from the OPRD model specification in one critical aspect, which is that the JSRD assumes complete population closure within primary occasions (i.e., no individuals can enter or leave), whereas the OPRD relaxes the closure assumption to allow individuals to geographically move into and out of the observable population within a primary occasion but retains a demographically closed population (i.e., no births or deaths; Kendall and Bjorkland 2001).

The underlying states ( $\Psi$ ) in the process model represent (1) individuals that have not entered the observable population; (2) alive, and

Table 2. State transitions ( $\Psi$ ) between time steps ( $i$ ) in the Jolly–Seber robust design model as a function of entry ( $b$ ), site persistence or apparent survival ( $\phi$ ), temporary emigration ( $\gamma''$ ), and re-immigration ( $\gamma'$ ) probabilities.

	$\Psi_{1_{i+1}}$	$\Psi_{2_{i+1}}$	$\Psi_{3_{i+1}}$	$\Psi_{4_{i+1}}$
$\Psi_{1_i}$	$1 - b_i$	$b_i$	0	0
$\Psi_{2_i}$	0	$\phi_i \times \gamma''_i$	$\phi_i \times (1 - \gamma''_i)$	$1 - \phi_i$
$\Psi_{3_i}$	0	$\phi_i \times \gamma'_i$	$\phi_i \times (1 - \gamma'_i)$	$1 - \phi_i$
$\Psi_{4_i}$	0	0	0	1

currently in the observable population; (3) alive, previously entered, but currently not in the observable population; and (4) permanently absent from, or otherwise not associated with the population (dead, permanent emigrant; Table 2).

For these exercises, we considered temporary emigration to be a completely random process (Kendall and Bjorkland 2001), but temporary emigration can also be modeled as a Markovian (i.e., state conditional) process. Observations of the state process matrix are relatively straightforward as only one of the four states needs to be partially observable (Table 3). We provide an assessment of model fit and parameter identifiability, and tools for simulating data for the JSRD and the full model parameterization in Appendix S1.

### Data structure

The approach presented here summarizes the individual-level observation model to the group-level to ensure detection is conditional on availability (Huggins 1991). This approach reduces model run duration, but it loses the ability to fit individual-level covariates on the observational

Table 3. Assignment of individuals to unobservable states (pre-entry, temporarily absent, permanently absent from study area) can be determined solely by observations of individuals within the study area conditioned on the ability to estimate a true detection probability ( $p^*$ ).

Variable	1	2	3	4
Seen	0	$p_i^*$	0	0
Not seen	1	$(1 - p_i^*)$	1	1

process. Although not presented in this manuscript, we provide model code for a parameterization of the JSRD that allows for individual-level information in Appendix S1. The data required for this model parameterization are the (1) encounter history; (2) detection matrix (DM); and (3) non-detection matrix (NDM). The encounter history used for this model is a matrix with, in its simplest form, dimensions  $n \times i$  written in the multistate notation used in other unobservable state demographic models (Kéry and Schaub 2012), in which one classification (e.g., state 1) represents an observation of an individual (1, 2, ...,  $n$ ) in a primary occasion ( $i$ ), and the other classification (e.g., state 2) represents the lack on an observation in a primary occasion. The DM, in its simplest form, the dimensions  $i \times j$ , represents the number of individuals observed in sample  $j$  in primary period  $i$  that were also observed in another sample during primary period  $i$ . For situations with two samples per primary period, the value imputed into the DM would be identical for each sample in primary period and would be the sum of the number of individuals seen in both occasions. The NDM, in its simplest form, the dimensions  $i \times j$ , represents the number of individuals not observed in sample  $j$  in primary period  $i$  but were observed (i.e., available for detection) in another sample during primary period  $i$ . In a two-sample scenario, the number of individuals with the capture history 01 would be assigned to the first sample of the NDM, and the number of individuals with the capture history 10 would be assigned to the second sample within a single primary of the NDM. Example R code to calculate these matrices from individual capture histories is provided in Appendix S1.

Unique to this parameterization, unbiased detection probabilities for each sample period

( $p_j$ ) during primary occasion  $i$  are estimated by assuming that the DM relative to all detections (i.e., DM + NDM) is distributed as a random binomial variable. This constraint ensures that detection probabilities are drawn from a distribution of individuals that were available for detection, which is a fundamental assumption for the robust design model.

$$DM_{i,j} \sim \text{binomial}(p_{i,j}, DM_{i,j} + NDM_{i,j})$$

$$p_{i,j} \sim \text{uniform}(0, 1)$$

Lastly,  $p_i^*$  is derived from the same equation used in maximum-likelihood approaches (Kendall et al. 1997).

$$p_i^* = 1 - \left( \prod_{j=1}^J (1 - p_{i,j}) \right)$$

Similar to other Bayesian implementations of Jolly–Seber models (Kéry and Schaub 2012, Lyons et al. 2016), we used the parameter expanded data augmentation approach (Royle and Dorazio 2012) to estimate the true number of marked individuals for each model iteration.

#### Simulation study

We developed a series of scenarios (Table 4) that varied in the underlying temporal variability of the simulated data and, correspondingly, model complexity, and considered time-constant, fixed temporal variation, and shrinkage or random time variation on estimated parameters. Additionally, we considered three levels of realistic sizes of the marked population ( $\hat{N} = 250, 500, \text{ or } 1000$  individuals) for demographic studies.

Table 4. List of model structures fit to simulated data to assess parameter bias and identifiability in the Jolly–Seber robust design model.

Model	$\beta$	$\phi$	$\gamma''$	$\gamma'$	$p^{1,2}$
1	$t$	.	.	.	$t$
2	$t$	$t$	.	.	$t$
3	$t$	$t$	$t$	.	$t$
4	$t$	$t$	$t$	$t$	$t$

Notes: Individual models within the model set varied in whether it allowed for temporal variation ( $t$ ) in each estimated parameter or constrained to be constant across time (.). Estimated parameters include ( $\beta$ ) entry, ( $\phi$ ) apparent survival ( $\gamma''$ ), temporary emigration, ( $\gamma'$ ) re-immigration, and ( $p$ ) sample (secondary) detection probabilities.

The mean and variance surrounding each model parameter used to simulate data sets were held constant for each data simulation and scenario (Appendix S1: Table S1). Normally distributed parameters were allowed to vary among data sets and, depending upon the scenario, occasions. Entry probabilities ( $b$ ) were drawn from a Dirichlet distribution (the multivariate generalization of the beta distribution; Hobbs and Hooten 2015) to (1) allow for an adequate number of individuals to enter the data set on the first occasion and (2) constrain the entry probabilities to sum to 1.0 across all seven occasions. Lastly, the true number of marked individuals available for capture for each data set (i.e., the marked superpopulation) was drawn from a Poisson distribution around a  $\lambda$  of 250, 500, or 1000 depending on the scenario.

*Parameter identifiability.*—We fit each simulated data set to a JSRD model and followed guidelines described in Gimenez et al. (2009) to assess the extent to which individual parameters were identifiable. We used the MCMCvis package (Youngflesh 2018) in R to calculate the percent overlap ( $\tau$ ) between the marginal prior distribution and marginal posterior distribution at each estimated parameter. We considered  $\tau < 0.35$  to indicate a parameter was identifiable, whereas  $\tau > 0.35$  was suggestive of parameters that were, at best, weakly identifiable (Garrett and Zeger 2000).

*Bias assessment.*—Next, we extracted and compared parameter estimates (and their variance) with the true value for each occasion in an encounter history to assess overall parameter fit. We reported the mean error (ME) and root-mean-squared error (RMSE), where  $n$  = the number of simulated trials, and  $x^i$  and  $\mu^i$  represented the parameter estimate and true parameter value from the  $i$ th trial, respectively. We used ME as a measure of bias for each parameter, whereas RMSE was used as a measure of precision. Model parametrization, priors, and data simulation code can be found in Appendix S1.

$$\text{ME} = \frac{1}{n} \sum_{i=1}^n (x^i - \mu^i)$$

$$\text{RMSE} = \sqrt{\frac{1}{n} \sum_{i=1}^n (x^i - \mu^i)^2}$$

*Simulation model specifications.*—We specified each demographic model within R (R Core Team

2012) with the package jagsUI to call JAGS (Plummer 2003). Each scenario/sample size combination ( $N = 12$  scenarios) comprised 100 simulated data sets based on the aforementioned parameter constraints (Appendix S1: Table S1). We opted to run short chains to increase the number of simulations we could run in a reasonable timeframe. After we assessed the performance of a series of exploratory model runs, we ran three chains of 2500 iterations ( $\text{thin} = 1$ ) with adapt and burn-in periods of 1000 and 500 iterations, respectively, for each simulated data set. Although model convergence often was not observed during these short-run lengths, exploratory assessments of the differences between these short-run parameter estimates and estimates drawn from the posteriors of longer model chains ( $>100,000$  iterations) were not substantial.

### Model application

*Monitoring.*—We applied the JSRD model to assess the impact of Hurricane Matthew on a population of non-breeding American oystercatchers in coastal Georgia from 2016 to 2017 and to confirm the real-world applicability of the model. We surveyed roosting habitats associated with the Altamaha Sound (AS) located in coastal Georgia, USA (Fig. 1), where previous monitoring efforts observed high use by non-breeding American oystercatchers. Surveys were timed to occur within two hours on either side of high tide to maximize detectability. Observers visited and surveyed all potential habitats within AS approximately every two to four weeks during the non-breeding season (August–April) of 2016–2017. These surveys encompassed both seasonal migrations and the overwintering period for American oystercatchers. We attempted to conduct paired surveys at each site that occurred on concurrent days (i.e., secondary sample) during each site visit (i.e., primary period). Typically, paired surveys occurred within one day of each other (median: 1; sd: 1.86 day(s)). If temporally adjacent surveys were greater than a week apart, we considered them a different primary occasion. Primary occasions were, on average, 20 d apart (range: 7–39 d). Each survey consisted of researchers (1) counting all observed American oystercatchers and classifying them as banded, unbanded, or of unknown band status and (2)

recording the unique band combinations on all banded birds when possible. Researchers also took high-resolution photographs of American oystercatchers to facilitate band identification and to classify a subset of individuals within each flock as subadults or adults through plumage and bill color characteristics associated (Prater et al. 1977).

*General model parameterization.*—We analyzed data collected from AS in a JSRD model to assess the impacts of Hurricane Matthew on American oystercatchers. We constrained demographic parameters at most time steps to be drawn from a normal distribution centered around a global mean ( $\bar{\mu}$ ) with a variance ( $\sigma$ ) specific to each demographic rate of interest to account for temporal variation. However, we allowed estimates for each demographic rate during the occasion immediately prior to and after Hurricane Matthew to estimate independently from all other occasions. Lastly, we allowed probabilities of detection for each sample during each occasion to be independent from each other. When weather or other logistical issues prevented observers from completing the necessary repeated survey ( $N = 3$ ), we fixed the detection period in the secondary sample occasion for that site to 0.

*Age-class ratios.*—Accurate assignment of American oystercatchers into discrete age classes is difficult to accomplish in large, dense flocks during surveys. Thus, we opted to take photographs randomly of partial flocks of American oystercatchers during each survey and assign individuals into age classes from these photographs. The field markings required for accurate age classification are associated with an individual's head and bill; thus, only individuals with those parts visible were classified as either adults or subadults. Each photograph was scored independently by two observers that recorded the total number of heads, adults, and subadults visible from the photograph. We built a mixture model to predict the age classes of unknown aged individuals based on the observed adult and juvenile ratios within each flock. We assumed the probabilities of being classified as either an adult or subadult from the photographs were (1) distributed as categorical random variables and that (2) unclassified individuals were random subsets of the flock relative to age class.

$$\text{age}_{1:i,f,s} \sim \text{categorical}(\pi_{1:A,f,s})$$

where age represented a vector of discrete age classifications ( $A$ ; adults, subadults) of  $i$  length, in which  $i$  represents number of individuals observed (i.e., adults, subadults, and unclassified) in each photograph  $f$  by each observer  $s$ , and  $\pi$  represented the estimated proportion of individuals in each picture classified in age-class  $A$ . As the goal of this model was to estimate the age classifications of unclassified individuals, the summed probability of being either an adult  $\pi_2$  or subadult  $\pi_1$  in each photograph was constrained to equal 1. In this scenario, we constrained  $\pi_{2,f,s}$  to be drawn from a normal distribution centered around the mean adult age-ratio  $\mu_{f,s}$ , which was informed by a linear model that considered that additive effects of site, primary occasion, and observer, with a variance ( $\sigma$ ). We then integrated the age-ratio model into the OPRD model to derive age-specific estimates of local abundance for each primary occasion.

$$\text{logit}(\pi_{2,f,s}) \sim \text{normal}(\mu_{f,s}, \sigma)$$

$$\pi_{1,f,s} = 1 - \pi_{2,f,s}$$

$$\mu_{f,s} = \beta_0 x_{\text{site}} + \beta_1 x_{\text{prim}} + \beta_2 x_{\text{obs}}$$

*Derived parameters.*—Modeling population demographic processes in a Bayesian framework offers the flexibility to estimate other derived quantities and their associated error. For this analysis, we used the estimated ratio of banded to total individuals from survey flock counts to adjust the estimated number of banded individuals into an estimate of the overall (i.e., banded and unbanded) population size, as demonstrated by Lyons et al. (2016). Similar to Lyons et al. 2016, estimates of stopover duration (i.e., the total duration an individual is within the observable population) and duration of absence (i.e., the total duration an individual is alive, but in the unobservable population) can be derived (see Appendix S1). Additionally, although our survey observations were frequent, interval length varied because of logistical issues; therefore, we corrected for interval length by deriving daily and weekly probabilities of each demographic rate. We reported the median value of the posterior distribution and standard

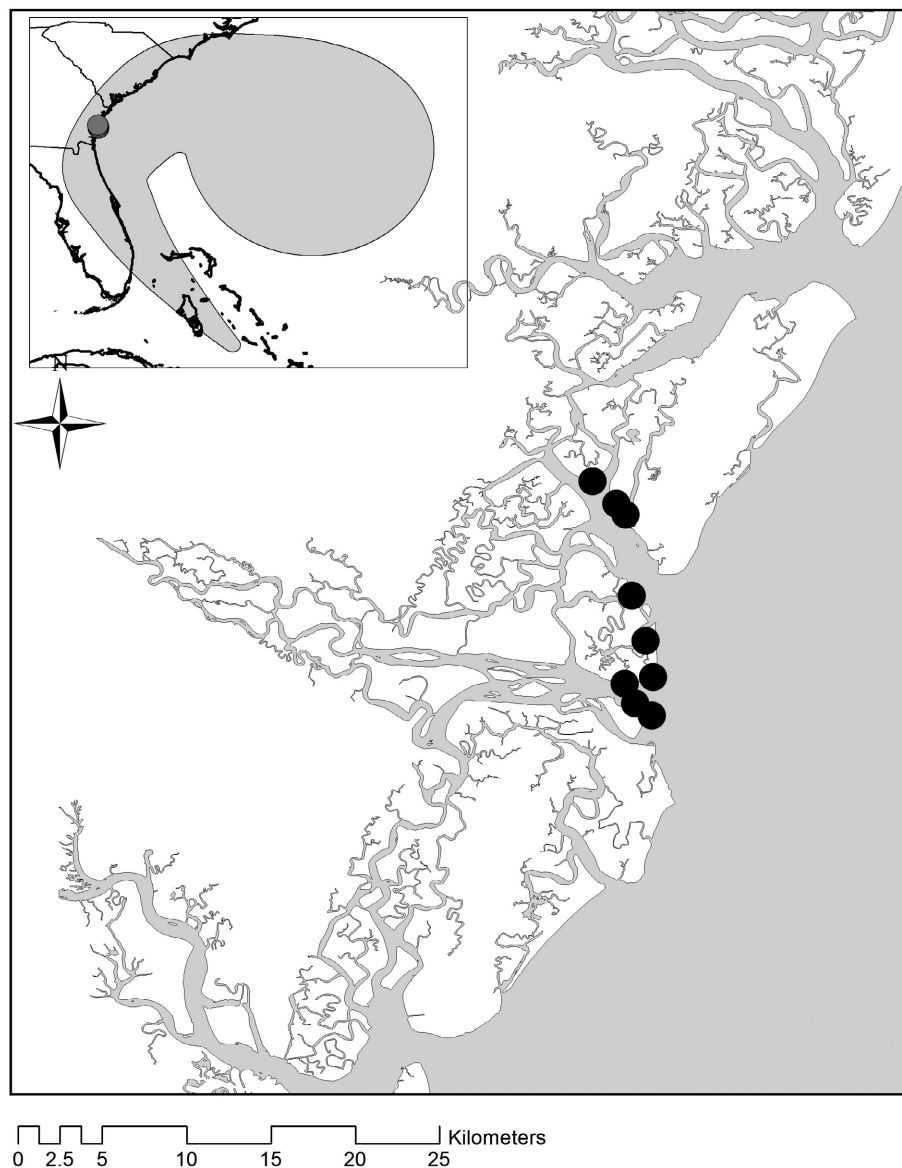


Fig. 1. Map of general flock locations surveyed for American oystercatchers near the Altamaha Sound (black circles) in coastal Georgia, USA. Inset map represents the modeled trajectory of Hurricane Matthew through the southern Atlantic Ocean from 4 October to 10 October 2016, passing over the study system (gray circle) on 8 October.

deviation of important parameters unless otherwise noted.

*Application model specifications.*—We specified our model within R (R Core Team 2012) with the package jagsUI to call JAGS (Plummer 2003). We ran four chains of 75,000 iterations (thin = 1) with adapt and burn-in periods of 25,000 iterations each.

*Goodness of fit.*—Following model convergence, we performed a posterior predictive check (Conn et al. 2018), in which we simulated replacement data sets based on parameter values from posterior distributions of our converged model that were relevant to each sub-model (i.e., CMR, age-ratio model, band ratio model) and determined whether these simulated data sets were different

from the observed data that informed each model. We reported Bayesian  $p$ -values based on comparisons between the estimated Freeman–Tukey statistic (Kéry and Schaub 2012) for both the observed and simulated data sets, in which Bayesian  $p$ -values near 0.5 indicate goodness of fit and values that approach 0.0 or 1.0 indicate lack of fit. We also assessed whether estimated parameters were fully identifiable by examining correlations among parameters based on the MCMC output (Gimenez et al. 2009) from the converged model. We considered pairs of parameters that either had

a Pearson's correlation value ( $r$ )  $>0.50$  or  $<-0.50$  to indicate that the parameters were not completely identifiable from one another.

## RESULTS

### Simulation results

Overall, results from the simulated scenarios indicated that parameter estimates from this model were generally identifiable (Fig. 2), unbiased, and sufficiently precise (Fig. 3; Appendix S1: Figs. S1–S12) under realistic sample size

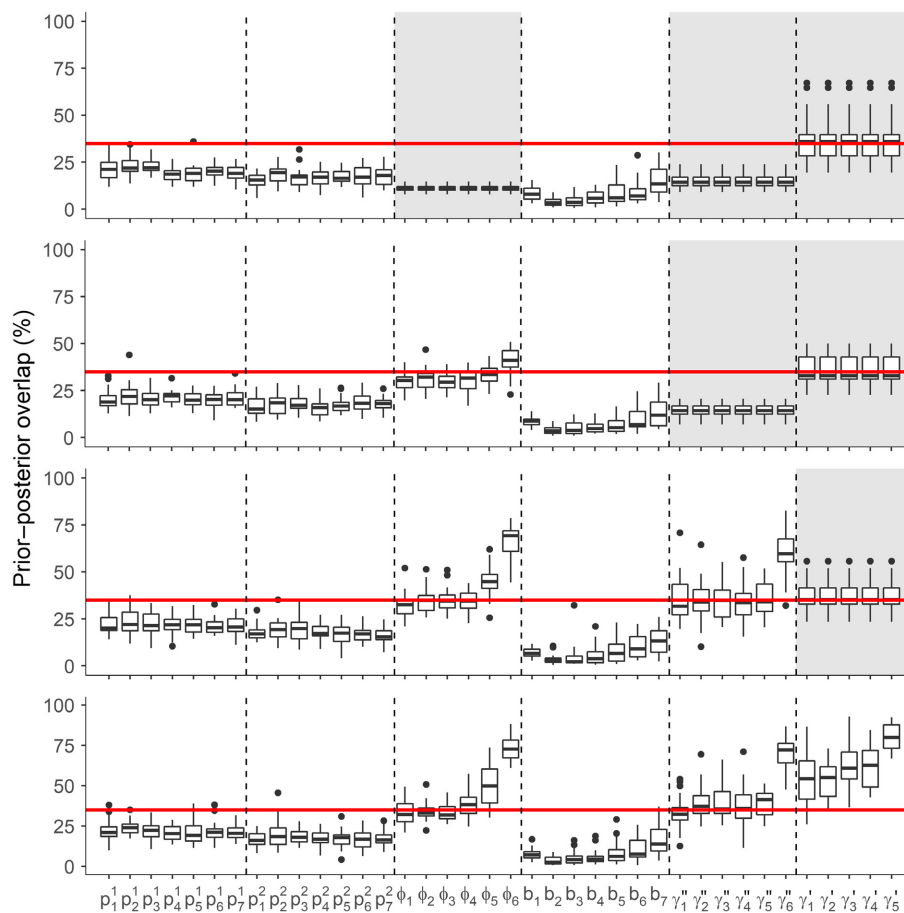


Fig. 2. The proportion of overlap between the marginal prior and posterior distributions (PPO) for each estimated parameter in the Jolly–Seber robust design model under varying levels of model complexity (white panels represent parameters that were allowed to vary among occasions (subscripts); gray panels represent parameters that were constrained to be constant across occasions). Box plots depict the median and distribution of PPO values observed across 100 simulated data sets. Values below the red line (0.35) were indicative of identifiable parameters (Gimenez et al. 2009), whereas values above the red line were indicative of parameters that were either weakly or non-identifiable. Parameters included detection during both secondary samples ( $p^1$ ,  $p^2$ ), apparent survival ( $\phi$ ), entry rates ( $b$ ), temporary emigration ( $\gamma''$ ), and re-immigration rates ( $\gamma'$ ).

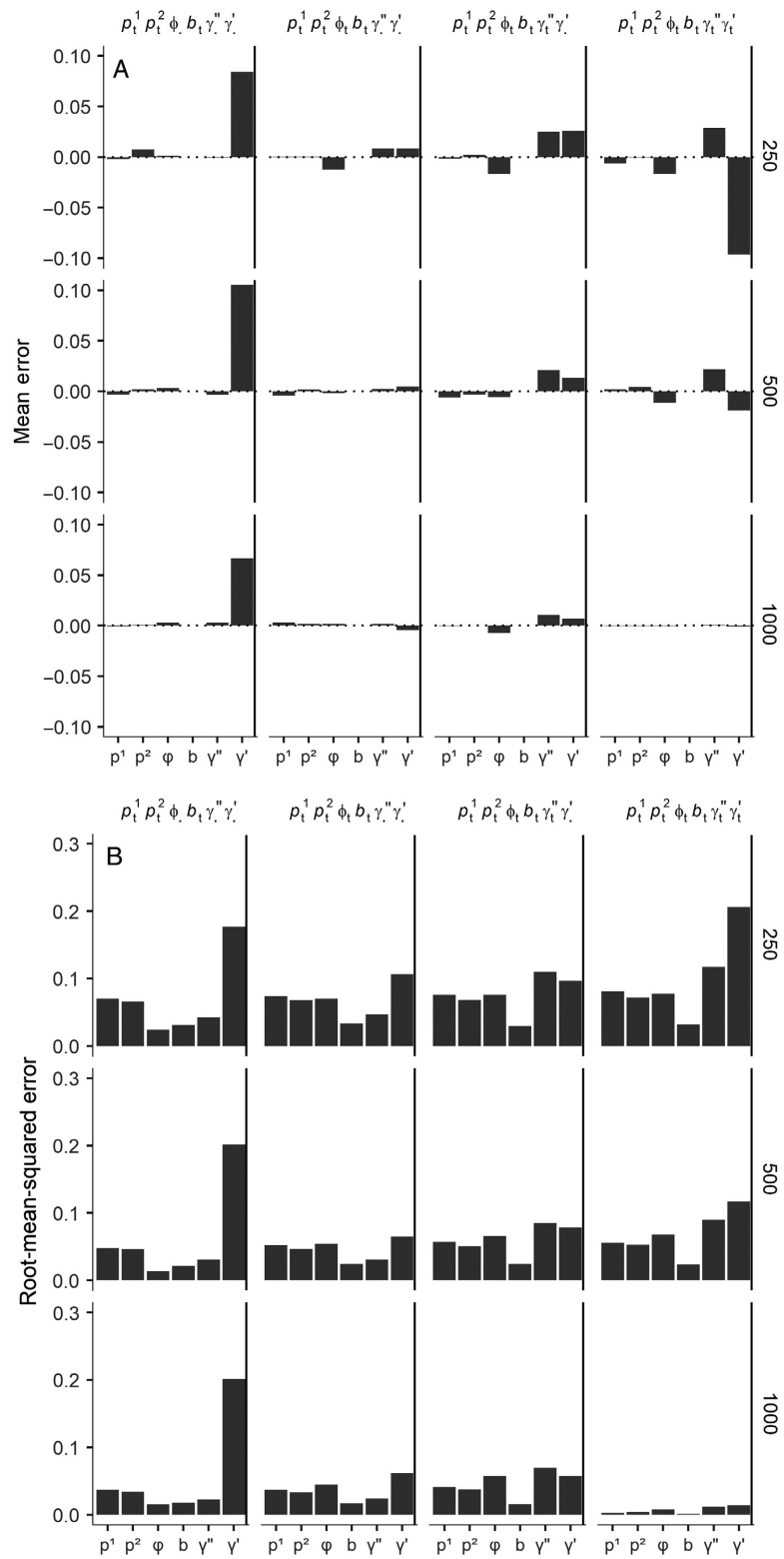


Fig. 3. The observed mean error (A) and root-mean-squared error (B) between estimated and simulated

(Fig. 3. *Continued*)

parameters (Table 1) from Jolly–Seber robust design models across 100 trials for four scenarios that varied in temporal model complexity ( $t$ : time specific;  $(.)$ : time constant) and sample size (250, 500, and 1000). Parameters included detection during both secondary samples ( $p^1, p^2$ ), apparent survival ( $\phi$ ), entry rates ( $b$ ), temporary emigration ( $\gamma''$ ), and re-immigration rates ( $\gamma'$ ).

and vital rate conditions. The re-immigration parameter ( $\gamma'$ ) was the least precise and, relatively, most biased parameter estimated. Estimates of  $\gamma'$  fit the data poorly in the least parameterized models, but improved slightly as overall model complexity increased. However, full-time variation on the  $\gamma'$  led to parameter estimates that were weakly identifiable, which suggested that interpretations of re-immigration rates in a fully expressed model should be limited. Additionally, parameter identifiability in the terminal periods for both the  $\phi$  and  $\gamma''$  parameters was reduced in fully time-expressed models.

In general, precision declined as model complexity increased. Although precision improved with increased sample size, parameter estimates were largely unbiased even at low sample sizes (Fig. 3). At lower sample sizes, estimates of  $\gamma''$  tended to be more biased in more complex models, but this bias was negligible in the 1000 individual scenario. All other parameters in this model (i.e.,  $\phi, \beta, p_s, p^*$ ) across sample size scenarios were both extremely precise and accurate. Interestingly, in the 1000 individual scenarios, parameter estimates remained unbiased even where parameters were determined to be weakly identifiable.

#### Application results

*Model validation.*—Posterior predictive checks for each sub-model (CMR: Bayesian  $p = 0.41$ ; age ratios: Bayesian  $p = 0.53$ ; band ratios: Bayesian  $p = 0.49$ ) indicated that data simulated from each predictive model was sufficiently similar to the observed data that informed each model. The majority of parameters estimated from the JSRD model were independent from one another, indicating they that were generally identifiable (Fig. 4). However, parameters associated with terminal occasions or occasions in which surveys were only performed during one of the secondary periods (i.e., occasions 4, 11, and 12) were

partially correlated with other and suspected to not be completely identifiable.

*Model results.*—From August 2016 through April 2017, we identified 241 uniquely banded American oystercatchers on AS. The largest number of American oystercatchers counted in a single flock during this time was 224 individuals. Detection probabilities ( $p$ ) at AL were generally high, but variable among (seasonal range: 0.41–0.88) and within primary occasions (range of differences in  $p$  within a primary: 0.08–0.27). True detection ( $p^*$ ) probabilities were high ( $\bar{p}^* = 0.84 \pm 0.05$ ) and more precise and consistent (range: 0.75–0.90) than estimates of  $p$ .

Estimates of weekly apparent survival ( $\phi_w$ ) were lower during the month prior to Hurricane Matthew (occasions 2 and 3:  $\phi_w = 0.945 \pm 0.020$ ;  $0.933 \pm 0.023$ ) relative to the occasion that overlapped Hurricane Matthew ( $\phi_w = 0.987 \pm 0.010$ ; Fig. 5A). We also observed that weekly probabilities of remaining in the observable population ( $\gamma''_w$ ) declined immediately prior and during Hurricane Matthew (occasions 3 and 4:  $\gamma''_w = 0.909 \pm 0.041$ ;  $0.907 \pm 0.040$ ; Fig. 5B) relative to prior to (occasion 2:  $\gamma''_w = 0.959 \pm 0.023$ ) or after (occasion 5:  $\gamma''_w = 0.972 \pm 0.018$ ) the hurricane event. Additionally, weekly conditional entry probabilities ( $b_w$ ) declined immediately before Hurricane Matthew (occasion 3:  $b_w = 0.017 \pm 0.008$ ) relative to the occasions before (occasion 2:  $b_w = 0.058 \pm 0.013$ ) or after (occasion 4:  $b_w = 0.047 \pm 0.012$ ; Fig. 5C). Lastly, weekly re-immigration rates ( $\gamma'_w$ ) were relatively invariant prior to and during Hurricane Matthew ( $\gamma'_w = 0.183$ – $0.197$ ) but increased following the hurricane ( $\gamma'_w = 0.346 \pm 0.146$ , Fig. 5D). Together these estimates indicated that (1) more individuals permanently left AS prior to Hurricane Matthew than during it; (2) more individuals temporally left AS during Hurricane Matthew than surrounding periods; (3) migration rates into AS temporarily declined prior to the Hurricane; and (4) re-immigration rates back into AS substantially increased following Hurricane Matthew.

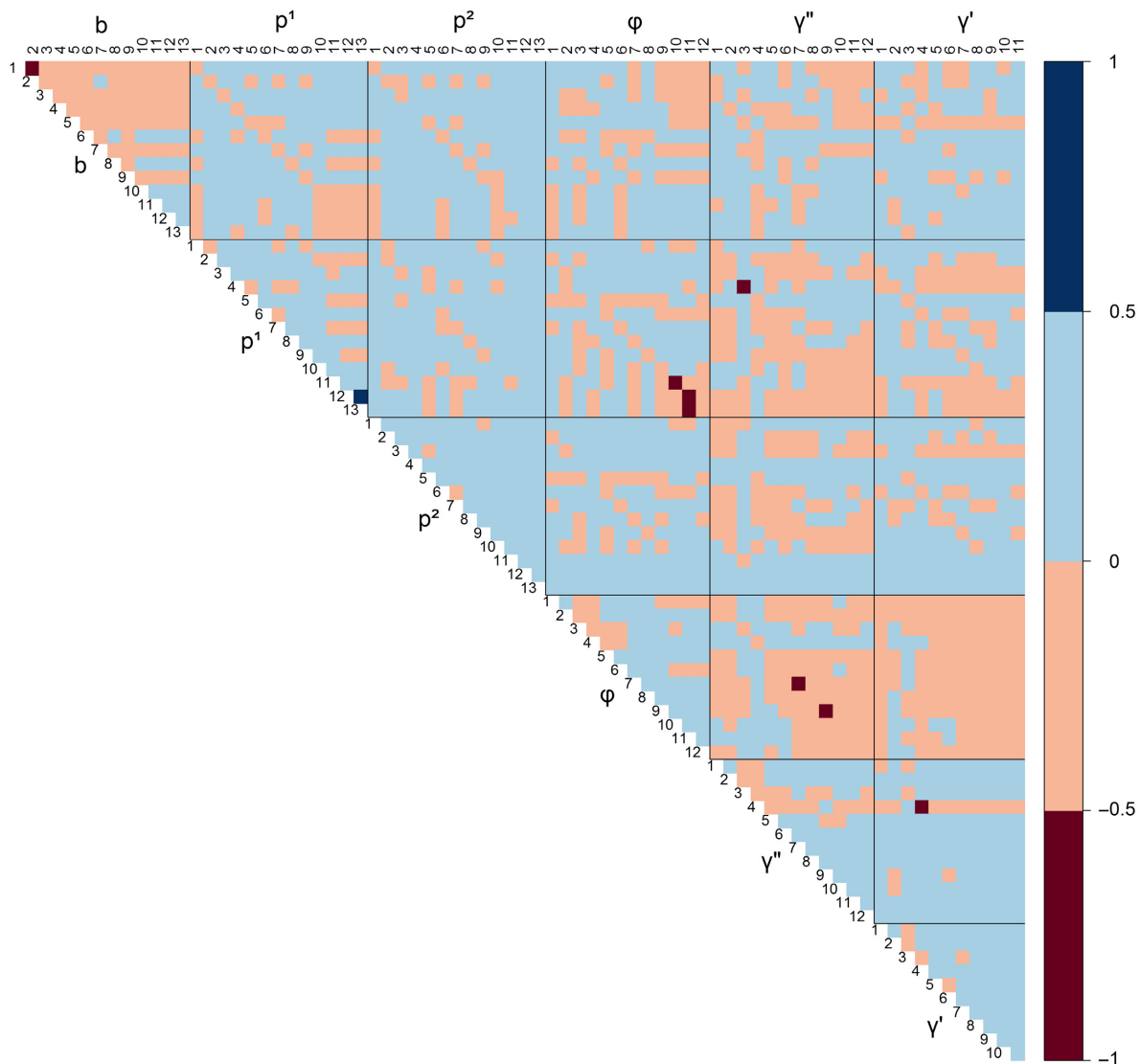


Fig. 4. Observed correlations between MCMC outputs for all estimated parameters in the American oystercatcher application of the Jolly–Seber robust design model. Parameters with a Pearson’s  $r$  correlation coefficient  $>0.5$  (dark blue) or  $<-0.5$  (dark red) were considered to be correlated and not fully identifiable from another. Grid lines delineate separate types of parameters, which included entry rates ( $b$ ), detection rates during both secondary samples ( $p^1$ ,  $p^2$ ), apparent survival ( $\phi$ ), temporary emigration ( $\gamma''$ ), and re-immigration rates ( $\gamma'$ ). Axis labels (1:13) indicate the time periods compared for each parameter. The diagonal was omitted for clarity.

These shifts in demographic rates resulted in an immediate reduction in local population abundance at AS prior to Hurricane Matthew (Fig. 6A) as individuals moved out of observable population (Fig. 6B), which was not compensated for by increased recruitment of immigrants (Fig. 6C). However, after the passage of the hurricane, the local population at AS rebounded as

recruitment of new individuals and re-immigration of previous entrants increased. We estimated that 881 (95% C.I.: 805–972) American oystercatchers used AS from August 2016 to April 2017, and 363 (95% C.I.: 293–449) individuals were on or near the site as Hurricane Matthew approached. Temporary emigrants, on average, only spent 13.09 (95% C.I.: 5.34–36.39) d away

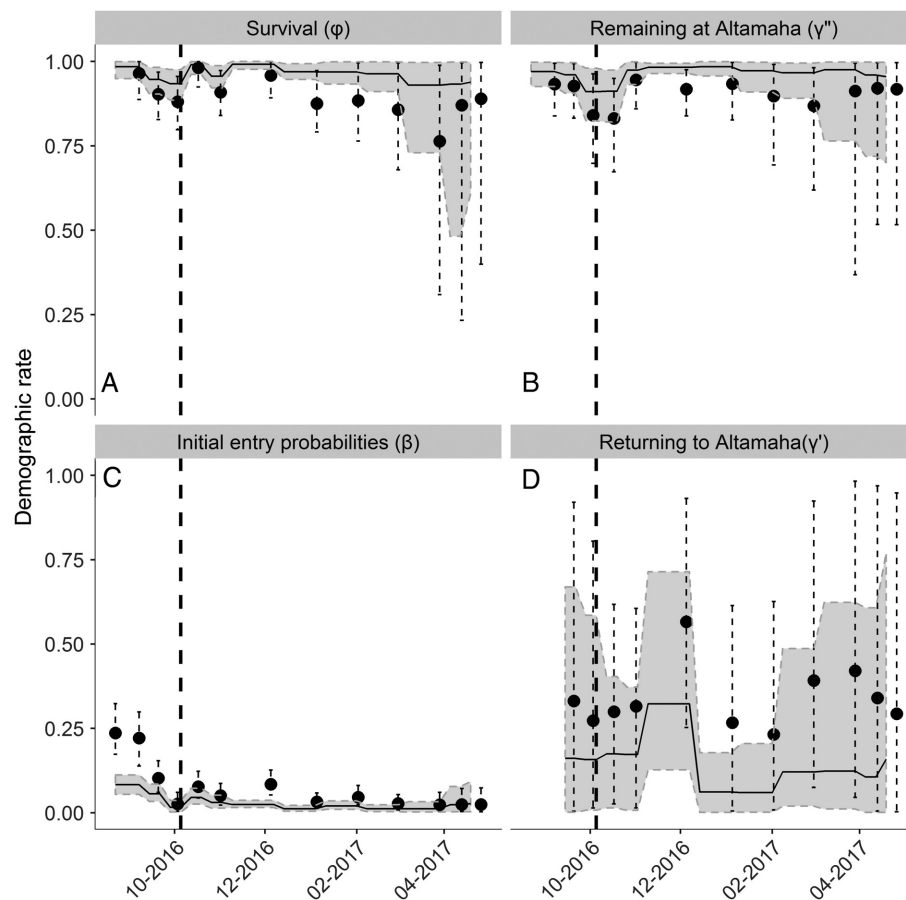


Fig. 5. Estimated occasion-specific (circles with error bars) and weekly (line with error bands) probabilities of (A) apparent survival ( $\phi$ ); (B) remaining on Altamaha Sound (AS;  $\gamma''$ ); (C) originally entering AS ( $\beta$ ); and (D) returning to the AS ( $\gamma'$ ) for American oystercatchers associated with AS in coastal Georgia, USA, from August 2016 to April 2017. Dotted vertical line represents when Hurricane Matthew struck coastal Georgia. Error bars and bands represent 95% Bayesian credible intervals.

from AS, as opposed to 87.70 (95% C.I.: 78.76–97.64) d at AS.

The estimated age-class ratio at AS was adult-centric with approximately 80% of the population classified as an adult ( $\bar{\pi}_A = 0.80$ ; 95% C.I.: 0.75–0.83), generally becoming more adult-biased (per period  $\Delta\bar{\pi}_A = 0.02$ ) throughout the non-breeding season. Integration of estimates of age ratios with the JSRD model also allowed us to derive site and age-class specific estimates of local abundance through the duration of the study. This model suggested that the decline in abundance at AS during the hurricane primarily was driven by a substantial reduction in subadult abundance, whereas adult abundance remained relatively

stable (Fig. 6D). Following the hurricane, adult abundance increased, whereas subadult abundance did not rebound, potentially indicative of permanent population losses.

## DISCUSSION

Despite the potential for a large mortality event, we found that American oystercatcher apparent survival was relatively high following the hurricane. Although we could not fully decouple true survival from permanent emigration in this analysis, the timing of the population losses suggested that mortality associated with Hurricane Matthew was relatively low and was experienced by

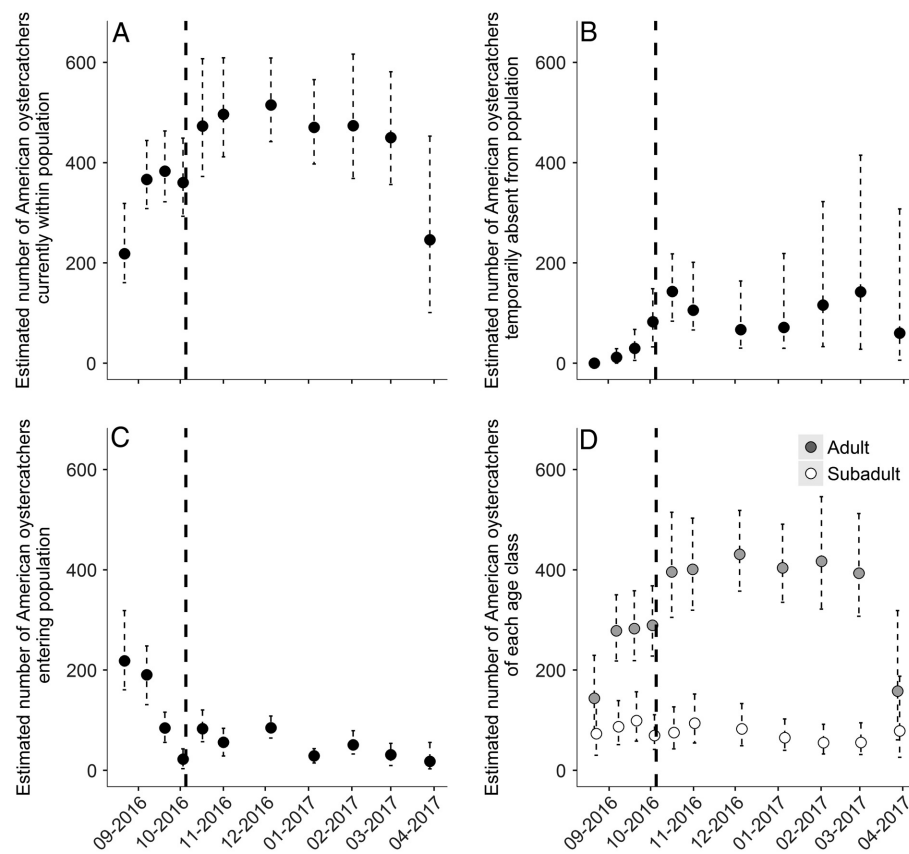


Fig. 6. Estimated number of American oystercatchers currently (A) on the Altamaha Sound (AS;  $N''$ ); (B) off AS ( $N'$ ), conditioned on entering on a previous occasion; (C) entering (B) the AS; and (D) the estimated number adults (gray circles) and subadults (white circles) in coastal Georgia, USA, from August 2016 to April 2017. Dotted vertical line represents when Hurricane Matthew struck coastal Georgia. Error bars represent 95% Bayesian credible intervals.

subadults. Regardless of mortality, it is not certain that the shifts in abundance were in response to Hurricane Matthew or simply an artifact of migration dynamics as the hurricane coincided with the fall oystercatcher migration. However, as multiple types (entry rates, temporary, and permanent emigration) of movement rates were relatively variable immediately prior to or during Hurricane Matthew, we suggest it's evidence of a causal relationship. As entry rates into the AS temporarily declined immediately prior to Hurricane Matthew, we speculate that migrating American oystercatchers were aware of Hurricane Matthew and either paused their migration at more northern latitudes or migrated directly into the non-observable population (e.g., more protected inland sites) in response.

Although it is unclear whether or how organisms can predict extreme environmental events, the ability to detect and the behavioral responses to these disturbances are most likely shaped by species' life-history constraints. Extreme events have been associated with reduced activity or torpor in species less able to make large movements, such as the common toad (*Bufo bufo*) and sugar gliders (*Petaurus breviceps*; Grant and Halliday 2010, Nowack et al. 2015), whereas dispersal or movement events have been associated in more mobile species, such as blacktip sharks (*Carcharhinus limbatus*), golden-winged warblers (*Vermivora chrysoptera*), and Brown Dippers (*Cinclus pallasii*; Heupel et al. 2003, Streby et al. 2015, Hong et al. 2018). Here, we demonstrated that a subset of the population of American oystercatchers monitored

temporarily moved from the observable population prior to, or during Hurricane Matthew. We were not able to determine the direction or distance of these movements, but the sparseness of movements among monitored non-breeding habitat during this period suggested these individuals moved away from established American oystercatcher habitat within this region. Although we observed a non-trivial amount of movement out of our study system during the Hurricane, the vast majority of individuals appeared to remain within the study system and were able to survive through other mechanisms.

Hurricanes have been associated with immediate population declines of many coastal avian species (Yaukey 2008, Raynor et al. 2013), including American oystercatchers (e.g., Hurricane Hugo; Marsh and Wilkinson 1991). Although our results suggest that American oystercatchers in Georgia largely avoided the immediate potential demographic consequences of Hurricane Matthew, we cannot currently determine its long-term impacts on this population of American oystercatchers. Complicating matters, hurricanes may either create new habitat or promote the transition of vegetation-encroached shorelines into early successional communities that benefit coastal birds (Cohen et al. 2009, Convertino et al. 2011b, Schulte and Simons 2016). Thus, initial shifts in abundance related to the hurricane event are not necessarily indicative of shifts in local population growth. As our study is the first assessment of the immediate demographic consequences of Hurricane Matthew on shorebird populations, it currently remains unclear what the overall impacts of Hurricane Matthew were on coastal species. However, given the timing and path of the hurricane in relation to migratory shorebirds (Weithman et al. 2018), Hurricane Matthew had the potential to substantially impact multiple species of conservation concern. Moreover, coastal Georgia was impacted by Hurricane Irma the year following Matthew, which suggests that shifts in the timing, frequency, and magnitude of hurricane activity in the North Atlantic Ocean, or other extreme weather events, coupled with sea-level rise (Convertino et al. 2012) are threats to shorebird population sustainability (Sutherland et al. 2012).

*Analytical advancements.*—Although perfectly unbiased estimates for some parameters (i.e.,  $\gamma'$

and  $\gamma''$ ) were not achievable at low sample sizes ( $\hat{N} < 500$ ) and realistic model constraints, the bias we observed on all parameters was sufficiently lower than previously published robust design models (Rankin et al. 2016). Our assessment of parameter identifiability also highlighted potential issues as a function of model complexity. In fully time-expressed models, multiple parameters were weakly identifiable at the terminal periods of the encounter history, which is a ubiquitous issue in CMR models (Gimenez et al. 2009). We do not consider these weakly identifiable parameters as an issue with our parameterization of the robust design model, but as an issue with robust design model in general. As the parameters affected or number of affected time steps may vary as function of sample size and number of sample occasions of the study, model validation procedures (e.g., percent prior–posterior overlap, correlations among parameters) should be incorporated prior to model inference to determine system-specific weaknesses. Based our simulation exercises, however, we suggest that researchers should exercise caution when inferring patterns in re-immigration from  $\gamma'$  in robust design models in the absence of out-of-system data, as it continues to be the parameter most likely to suffer from identifiability issues.

The assumption of equal survival probabilities for individuals within and outside of the observable population remains a potential source of bias in this model parameterization (Kendall and Bjorkland 2001, Henle and Gruber 2017). However, building models that integrate other data-types that further explain the survival process (e.g., out-of-system observations, telemetry, harvest data) can relax this assumption, which is currently easier to accomplish in a Bayesian, than in a maximum-likelihood, framework due to its increased flexibility (Schaub and Abadi 2011). In that regard, the parameterization of our model was deliberately designed to be more easily implemented relative to previous robust design models (Rankin et al. 2016). Collapsing the detection process into a group-specific, as opposed to an individual-specific, process results in a substantial reduction in model run-time.

Following the approach for estimating stopover duration presented in Lyons et al. (2016), estimates of both stopover duration and duration of temporary absence were derived from this

model, which both can be of biological importance. The JSRD model presented here can quickly be modified to address system-specific questions. For example, this model can be expanded to include multiple observable sites and estimate movements among the observable and unobservable sites to investigate metapopulation dynamics (Chabanne et al. 2017). Most importantly, our approach of integrating estimates of overall abundance generated from resight data with estimates of age and band ratios from survey data (i.e., flock photographs) allowed for more descriptive and potentially less biased estimates of age-specific abundance, relative to estimates generated solely from either mark-resight or survey data. First, the JSPD model provided a mechanism to account for individuals temporarily leaving the observable population, which, if ignored, biases count-based estimates of abundance low (Chandler et al. 2011). Second, estimating age ratios from the survey data provided a mechanism to account for potential age-related biases in mark-resight data. For example, depending on a combination of the life-history characteristics and researcher methods, cohorts of individuals (e.g., subadults) may be underrepresented in CMR data due to an inability to adequately capture a representative subsample of these individuals, which may bias estimates of the age structure of a population if inference was based solely on the banding data.

## ACKNOWLEDGMENTS

Funding for this study was provided by the National Fish and Wildlife Foundation, Georgia Department of Natural Resources, and Virginia Polytechnic Institute and State University. We thank two anonymous reviewers for their comments on an earlier draft of this manuscript. We thank the Virginia Tech's Open Access Subvention Fund for providing funds for publication costs. We also thank G. DiRenzo for providing useful code.

## LITERATURE CITED

- Barker, R. J. 1997. Joint modeling of live-recapture, tag-resight, and tag-recovery data. *Biometrics* 53:666–677.
- Blomberg, E. J., J. S. Sedinger, D. V. Nonne, and M. T. Atamian. 2013. Annual Male Lek attendance influences count-based population indices of Greater Sage-Grouse. *Journal of Wildlife Management* 77:1583–1592.
- Boone, M. 2016. The effect of Hurricane Sandy on landbird migration in the northeastern United States. Thesis. University of Delaware, USA.
- Chabanne, D. B. H., K. H. Pollock, H. Finn, and L. Bejder. 2017. Applying the multistate capture–recapture robust design to characterize metapopulation structure. *Methods in Ecology and Evolution* 8:1547–1557.
- Chandler, R. B., J. A. Royle, and D. I. King. 2011. Inference about density and temporary emigration in unmarked populations. *Ecology* 92:1429–1435.
- Chu-Agor, M. L., R. Muñoz-Carpena, G. A. Kiker, M. Aiello-Lammens, R. Akçakaya, M. Convertino, and I. Linkov. 2012. Simulating the fate of Florida Snowy Plovers with sea-level rise: exploring potential population management outcomes with a global uncertainty and sensitivity analysis perspective. *Ecological Modelling* 224:33–47.
- Cohen, J. B., L. M. Houghton, and J. D. Fraser. 2009. Nesting density and reproductive success of piping plovers in response to storm- and human-created habitat changes. *Wildlife Monographs* 173:1–24.
- Conn, P. B., D. S. Johnson, P. J. Williams, S. R. Melin, and M. B. Hooten. 2018. A guide to Bayesian model checking for ecologists. *Ecological Monographs*. <https://doi.org/10.1002/ecm.1314>
- Convertino, M., J. Donoghue, M. Chu-Agor, G. Kiker, R. Munoz-Carpena, R. Fischer, and I. Linkov. 2011a. Anthropogenic renourishment feedback on shorebirds: a multispecies Bayesian perspective. *Ecological Engineering* 37:1184–1194.
- Convertino, M., J. B. Elsner, R. Muñoz-Carpena, G. A. Kiker, C. J. Martinez, R. A. Fischer, and I. Linkov. 2011b. Do tropical cyclones shape shorebird habitat patterns? *Biogeoclimatology of Snowy Plovers in Florida*. *PLoS ONE* 6:e15683.
- Convertino, M., P. Welle, R. Muñoz-Carpena, G. A. Kiker, M. L. Chu-Agor, R. A. Fischer, and I. Linkov. 2012. Epistemic uncertainty in predicting shorebird biogeography affected by sea-level rise. *Ecological Modelling* 240:1–15.
- Frederiksen, M., F. Daunt, M. P. Harris, and S. Wanless. 2008. The demographic impact of extreme events: Stochastic weather drives survival and population dynamics in a long-lived seabird. *Journal of Animal Ecology* 77:1020–1029.
- Garrett, E., and S. Zeger. 2000. Latent class model diagnosis. *Biometrics* 56:1055–1067.
- Gimenez, O., B. J. Morgan, and S. P. Brooks. 2009. Weak identifiability in models for mark–recapture–recovery data. Pages 1055–1067 *in* D. L. Thomson, E. G. Cooch, and M. J. Conroy, editors. *Modeling demographic processes in marked populations*. Environmental and ecological statistics. Volume 3. Springer, Boston, Massachusetts, USA.

- Grant, R. A., and T. Halliday. 2010. Predicting the unpredictable; evidence of pre-seismic anticipatory behaviour in the common toad. *Journal of Zoology* 281:263–271.
- Henle, K., and B. Gruber. 2017. Performance of multi-state mark-recapture models for temporary emigration in the presence of survival costs. *Methods in Ecology and Evolution* 9:657–667.
- Heupel, M. R., C. A. Simpfendorfer, and R. E. Hueter. 2003. Running before the storm: Blacktip sharks respond to falling barometric pressure associated with Tropical Storm Gabrielle. *Journal of Fish Biology* 63:1357–1363.
- Hobbs, N. T., and M. B. Hooten. 2015. Bayesian models: a statistical primer for ecologists. Princeton University Press, Princeton, New Jersey, USA.
- Hong, S.-Y., S. P. Sharp, M.-C. Chiu, M.-H. Kuo, and Y.-H. Sun. 2018. Flood avoidance behaviour in Brown Dippers *Cinclus pallasi*. *Ibis* 160:179–184.
- Huggins, R. M. 1991. Some practical aspects of a conditional likelihood approach to capture experiments. *Biometrics* 47:725–732.
- James, F. C., C. A. Hess, and D. Kufrin. 1997. Species-centered environmental analysis: indirect effects of fire history on red-cockaded woodpeckers. *Ecological Applications* 7:118–129.
- Keim, B. D., and R. A. Muller. 2007. Spatiotemporal patterns and return periods of tropical storm and hurricane strikes from Texas to Maine. *Journal of Climate* 20:3498–3509.
- Kendall, W. L., R. J. Barker, G. C. White, M. S. Lindberg, C. A. Langtimm, and C. L. Penalzoa. 2013. Combining dead recovery, auxiliary observations and robust design data to estimate demographic parameters from marked individuals. *Methods in Ecology and Evolution* 4:828–835.
- Kendall, W. L., and R. Bjorkland. 2001. Using open robust design models to estimate temporary emigration from capture–recapture data. *Biometrics* 57:1113–1122.
- Kendall, W. L., J. D. Nichols, and J. E. Hines. 1997. Estimating temporary emigration using capture–recapture data with Pollock’s robust design. *Ecology* 78:563–578.
- Kéry, M., and M. Schaub. 2012. Bayesian population analysis using WinBUGS: a hierarchical perspective. Academic Press, Waltham, Massachusetts, USA.
- Le Corre, M., C. Dussault, and S. D. Cote. 2017. Weather conditions and variation in timing of spring and fall migrations of migratory caribou. *Journal of Mammalogy* 98:260–271.
- Lebreton, J. D., K. P. Burnham, J. Clobert, and D. R. Anderson. 1992. Modeling survival and testing biological hypotheses using marked animals: a unified approach with case-studies. *Ecological Monographs* 62:67–118.
- Link, W. A., and R. J. Barker. 2010. Bayesian inference with ecological applications. Academic Press, Burlington, Massachusetts, USA.
- Lyons, J. E., W. L. Kendall, J. A. Royle, S. J. Converse, B. A. Andres, and J. B. Buchanan. 2016. Population size and stopover duration estimation using mark–resight data and Bayesian analysis of a superpopulation model. *Biometrics* 72:262–271.
- Marsh, C. P., and P. M. Wilkinson. 1991. The impact of Hurricane Hugo on coastal bird populations. *Journal of Coastal Research* 8:327–334.
- Muths, E., R. D. Scherer, P. S. Corn, and B. A. Lambert. 2006. Estimation of temporary emigration in male toads. *Ecology* 87:1048–1056.
- Nowack, J., A. D. Rojas, G. Kortner, and F. Geiser. 2015. Snoozing through the storm: torpor use during a natural disaster. *Scientific Reports* 5: 11243.
- Plummer, M. 2003. A program for analysis of Bayesian graphical models using Gibbs sampling. *in* 3rd International Workshop on Distributed Statistical Computing (DCS2003), Vienna, Austria.
- Pollock, K. H. 1982. A capture–recapture design robust to unequal probability of capture. *Journal of Wildlife Management* 46:752–757.
- Prater, A. J., J. H. Marchant, and J. Vuorinen. 1977. Guide to the identification and ageing of holarctic waders. Herts, Tring, UK.
- R Core Team (2018). R: a language and environment for statistical computing. R Foundation for Statistical Computing, Vienna, Austria. <https://www.R-project.org>
- Rankin, R. W., K. E. Nicholson, S. J. Allen, M. Krützen, L. Bejder, and K. H. Pollock. 2016. A full-capture hierarchical Bayesian model of Pollock’s closed robust design and application to dolphins. *Frontiers in Marine Science* 22:25.
- Raynor, E. J., A. R. Pierce, T. M. Owen, C. M. Leumas, and F. C. Rohwer. 2013. Short-term demographic responses of a coastal waterbird community after two major hurricanes. *Waterbirds* 36:88–93.
- Royle, J. A., and R. M. Dorazio. 2012. Parameter-expanded data augmentation for Bayesian analysis of capture–recapture models. *Journal of Ornithology* 152:S521–S537.
- Schaub, M., and F. Abadi. 2011. Integrated population models: a novel analysis framework for deeper insights into population dynamics. *Journal of Ornithology* 152:227–237.
- Schofield, M. R., and R. J. Barker. 2011. Full open population capture–recapture models with individual covariates. *Journal of Agricultural Biological and Environmental Statistics* 16:253–268.

- Schulte, S. A., and T. R. Simons. 2016. Hurricane disturbance benefits nesting American Oystercatchers (*Haematopus palliatus*). *Waterbirds* 39:327–337.
- Souchay, G., G. Gauthier, and R. Pradel. 2014. To breed or not: a novel approach to estimate breeding propensity and potential trade-offs in an Arctic-nesting species. *Ecology* 95:2745–2756.
- Sprogis, K. R., K. H. Pollock, H. C. Raudino, S. J. Allen, A. M. Kopps, O. Manlik, J. A. Tyne, and L. Bejder. 2016. Sex-Specific patterns in abundance, temporary emigration and survival of Indo-Pacific Bottlenose Dolphins (*Tursiops aduncus*) in coastal and estuarine waters. *Frontiers in Marine Science* 3:12.
- Stewart, S. R. 2017. Tropical cyclone report: Hurricane Matthew, September 28 – October 9, 2016. [https://www.nhc.noaa.gov/data/tcr/AL142016\\_Matthew.pdf](https://www.nhc.noaa.gov/data/tcr/AL142016_Matthew.pdf)
- Streby, H. M., G. R. Kramer, S. M. Peterson, J. A. Lehman, D. A. Buehler, and D. E. Andersen. 2015. Tornadoic storm avoidance behavior in breeding songbirds. *Current Biology* 25:98–102.
- Sutherland, W. J., et al. 2012. A horizon scanning assessment of current and potential future threats to migratory shorebirds. *Ibis* 154:663–679.
- Volkov, S. V., O. S. Grinchenko, and T. V. Sviridova. 2016. The effects of weather and climate changes on the timing of autumn migration of the common crane (*Grus grus*) in the north of Moscow region. *Biology Bulletin* 43:1203–1211.
- Weithman, C., D. Gibson, K. Hunt, M. Friedrich, J. Fraser, S. Karpanty, and D. Catlin. 2017. Senescence and carryover effects of reproductive performance influence migration, condition, and breeding propensity in a small shorebird. *Ecology and Evolution* 7:11044–11056.
- Weithman, C. E., D. Gibson, K. M. Walker, S. Maddock, J. D. Fraser, S. M. Karpanty, and D. H. Catlin. 2018. Discovery of an important stopover location for migratory piping plovers on South Point, Ocracoke Island, North Carolina. *Waterbirds* 42:56–62.
- White, G. C., W. L. Kendall, and R. J. Barker. 2006. Multistate survival models and their extensions in Program MARK. *Journal of Wildlife Management* 70:1521–1529.
- Yaukey, P. H. 2008. Effects of Hurricane Katrina on the urban resident landbirds of New Orleans, Louisiana. *Condor* 110:158–161.
- Youngflesh, C. 2018. MCMCvis: tools to visualize, manipulate, and summarize MCMC output. *Journal of Open Source Software* 3:640–643.

## SUPPORTING INFORMATION

Additional Supporting Information may be found online at: <http://onlinelibrary.wiley.com/doi/10.1002/ecs2.2334/full>